J Appl Electrochem (2014) 44:467–474
DOI 10.1007/s10800-013-0627-1

RESEARCH ARTICLE

The influence of carbon content on the lithium diffusion and electrochemical properties of lithium vanadium phosphate

Nils Böckenfeld · Andrea Balducci

Received: 14 July 2013 / Accepted: 14 September 2013 / Published online: 25 September 2013
© Springer Science+Business Media Dordrecht 2013

Abstract The influence of carbon content and porosity of lithium vanadium phosphate, $Li_3V_2(PO_4)_3$, on its diffusion properties and electrochemical performance was examined by GITT and galvanostatic charge/discharge experiments. The diffusion coefficient of $Li_3V_2(PO_4)_3$, as determined by GITT measurements, appears relatively high, thus making this material interesting also for high power application. Moreover, the results of this study clearly show that the porosity and the carbon content of the electrode materials is an important factor affecting the diffusion as well as the electrochemical performance of $Li_3V_2(PO_4)_3$. It was demonstrated that excessive carbon coating may lead to kinetic hindrances but may also contribute specific capacity in anode materials in voltage regions below 1.0 V versus Li/Li^+.

Keywords Lithium vanadium phosphate · Diffusion coefficient · Carbon

1 Introduction

Rechargeable lithium ion batteries (LIB) have become the most promising energy storage devices for electric and hybrid electric vehicles. In addition, they are now considered as buffer systems for intermittent renewable energy sources due to their high energy and power densities and long cycle lifetime [1, 2].

N. Böckenfeld · A. Balducci (✉)
MEET Battery Research Centre, Institute of Physical Chemistry, University of Münster, Corrensstraße 28/30, 48149 Muenster, Germany
e-mail: andrea.balducci@uni-muenster.de

Recently, lithiated transition metal phosphates, such as $LiMPO_4$ (M = Mn, Fe, Co, Ni) and $Li_3M_2(PO_4)_3$ (M = Ti, V, Fe) have attracted great interest as potential cathode materials for LIBs, because they have good electrochemical and thermal stabilities, competitive energy density and high operating potentials [3, 4]. The most prominent example is $Li_3V_2(PO_4)_3$ (LVP), which offers the optimal combination of high operating voltage, high specific capacity, good ionic mobility and excellent thermal stability [5–8]. $Li_3V_2(PO_4)_3$ can theoretically reversibly deliver 3 Li^+ per formular unit within the potential range comprising between 3.0 and 4.8 V versus Li/Li^+, which results in a maximum discharge capacity of 197 mAh g^{-1}. In the potential range between 3.0 and 4.3 V versus Li/Li^+, based on the $V^{3+/}V^{4+}$ redox couple, a reversible capacity of 131 mAh g^{-1} can still be obtained [6].

LVP is an amphoteric material. Therefore, it is also able to reversibly host additional lithium ions in its structure, thus working also as anodic material. In the voltage range between 3.0 and 0.0 V versus Li/Li^+, and between 3.0 and 1.0 V versus Li/Li^+, stable reversible capacities of about 250 and 100 mAh g^{-1}, respectively, have been observed [8, 9] The charge/discharge process proceeds via two-phase transitions in the voltage range between 3.0 and 1.6 V versus Li/Li^+, where four isotypic monoclinic phases occur in $Li_xV_2(PO_3)_4$ (x = 3.0, 3.5, 4.0, 4.5 and 5.0). After this sequence of phase transitions a solid-solution behavior is observed in the voltage range between 1.6 and 0 V versus Li/Li^+, which allows the uptake and release of additional lithium resulting in $Li_xV_2(PO_3)_4$ (x = 5.0–7.0).

To quantify the lithium diffusion coefficients of the material different techniques have been applied in the past. The lithium ion diffusion of the LVP as anode material has been experimentally probed by GITT, CV and EIS techniques [10]. Since the application of LVP as cathode

material seems to be even more promising, the lithium ion diffusion properties in this voltage and composition range have been addressed by means of different experimental techniques (GITT, CV, 1D ^{6}Li Selective Inversion NMR) as well as atomistic simulations [11–13].

The preparation method and especially the choice of reducing and carbon-coating agent are crucial to obtain LVP with distinct properties [9, 14–18]. The particle size, morphology, carbon content and carbon distribution play an important role since they influence the lithium ion diffusion and electronic conductivity of the material. For example, the variation of the carbon-coating precursor, e.g., citric acid, glucose or starch, has been shown to have a strong effect on the resistance, specific capacity as well as rate performance of the material [19]. High carbon content may improve the electronic conductivity, but could diminish the ionic conductivity. Therefore, for the realization of a high performance material, it is important to find a balance between these two factors.

In this work, we prepared three different LVP samples by sol–gel synthesis. By variation of the reducing agents (which also act as precursors for the carbon coating) the carbon content, morphology and surface area of the obtained materials were modified. All three compounds were electrochemically characterized as cathode as well as anode materials. In addition, also the lithium ion diffusion properties were investigated to verify the influence of carbon content and surface area on the practical diffusion characteristics of this material.

2 Experimental

2.1 Synthesis

Three different LVP samples were prepared via a sol–gel method using NH_4VO_3, $LiCH_3COO$ and $NH_4H_2PO_4$ (in a molar ratio of 2:3:3) as precursor. Citric acid (V:Li:PO_4:CA = 2:3:3:10), oxalic acid (V:Li:PO_4:OA = 2:3:3:6), and a mixture of citric and oxalic acid (V:Li:PO_4:CA:OA = 2:3:3:2:6) were used as reducing and chelating agents. Initially, NH_4VO_3 and the reducing agent (either citric or oxalic acid or a mixture of citric–oxalic acid) were dissolved in deionized water at 80 °C. Afterwards, a solution containing $LiCH_3COO$ and $NH_4H_2PO_4$ was prepared at 80 °C and added to the first one. The resulting solution was stirred at 80 °C to obtain a dark green gel, which was dried for 24 h under ambient atmosphere in an oven at 80 °C. The gel precursor was grinded with an agate mortar, transferred to a tube furnace and sintered under constant flow of Argon at 300 °C for 4 h with a heating rate of 5 °C min^{-1}. The resulting precursor was reground and then sintered under constant flow of Argon at 750 °C for 12 h with a heating rate of 10 °C min^{-1}. In the following, the LVP sample obtained using citric acid will be indicated as LVP/CA, the one using oxalic acid will be named LVP/OA, while the LVP sample obtained using the mixture of citric acid and oxalic acid will be indicated as LVP/CA+OA.

The lithium, vanadium and phosphorus content of the two LVP samples were determined by the inductively coupled plasma optical emission spectrometry (ICP-OES, SPECTRO ARCOS, Ametek, Germany). The crystalline structure was characterized by X-ray diffraction (XRD) using the Cu Kα radiation on the Bruker D8 Advance (Germany) in the 2θ range from 10° to 60°. The carbon and hydrogen content of the samples was evaluated by elementary CHN combustion analysis. The specific BET surface area of the active material particles was determined using the ASAP 2020 from Micromeritics Instrument Corporation (USA).

2.2 Electrode preparation and characterization

Composite electrodes containing LVP as an active material were prepared using a process similar to that reported in [20]. The composition of the dry electrodes was 85 % LVP, 10 % conducting agent (Super C65, TIMCAL) and 5 % binder polyvinylidene fluoride. The electrodes were coated on etched aluminum foil (5 wt% KOH, 60 °C, 30 s) or on dendritic copper foil. The electrode area was 1.13 cm^2. The electrode mass loading was about 0.8 mg cm^{-2}. The electrode density was 1.2 g cm^{-3}.

Electrochemical tests were carried out in Swagelok®-type 3-electrodes cells, which were assembled in an argon-filled glove box (H_2O <1 ppm, O_2 <1 ppm). For all experiments, a Whatman GF/D glass microfiber filter of 675 µm in thickness and 12 mm in diameter was used as a separator. The separator was drenched with 120 µL of 1 M $LiPF_6$ in ethylene carbonate/dimethyl carbonate (EC/DMC) 1:1.

The composite electrodes were tested in half-cell configuration, using metallic lithium as counter and reference electrodes. Cyclic voltammetries (CV) were performed using a VMP multichannel potentiostatic–galvanostatic system (Biologic Science Instrument, France). In the case of the composites electrodes coated on aluminum foil the CVs were carried out in the voltage range from 3.0 to 4.3 V versus Li/Li$^+$. In the case of the composites electrodes coated on copper foil the CVs were carried out in the voltage range from 3.0 to 0.0 versus Li/Li$^+$. For both voltage ranges, a scan rate of 0.05 mV s^{-1} was used. Constant current (CC) tests were performed applying charge–discharge currents ranging from C/2 to 10C. In the case of the cathodes a nominal capacity of 133 mAh g^{-1} was used for the calculation of the current densities. In the case of the anodes a nominal capacity of 550 mAh g^{-1} was

considered. Five full charge–discharge cycles were carried out for each considered C-rate. The cut-off potentials used for the CC tests were identical to that used for the CV test.

For the GITT experiments short current pulses of current densities corresponding to C-rates of C/10 were applied for 10 min, followed by a relaxation time of 1 h to allow the system to achieve electrochemical equilibrium. The diffusion coefficient of the investigated material was calculated using the equation:

$$D_{\mathrm{Li+}} = \frac{4}{\pi}\left(\frac{m_B V_m}{M_B A}\right)^2 \left(\frac{\Delta E_s}{\Delta E_\tau}\right)^2 \quad (1)$$

In this equation, M_B and m_B are the molecular weight (g mol^{-1}) and mass loading (g) of the active material (lithium host), V_M is the molar volume (mol cm^{-3}) of the compound which can be obtained from the volume of the unit cell, A is the electroactive surface area (contact area between active material and electrolyte) (cm^2) and τ (s) the time period for which the constant current is applied.

3 Results and discussion

The LVP samples were characterized by XRD diffraction and, as shown in Fig. 1, all of them (LVP/CA, LVP/CA+OA and LVP/OA) display the same monoclinic crystal structure with space group of P_{21}/n. These structures are in very good agreement with the lattice parameters already published [21]. Although all three materials display the same structure, their morphology is markedly different as can be seen from the SEM images reported in Fig. 2. As shown in the figure, the use of citric acid leads to the formation of LVP/CA particles with a size in the order

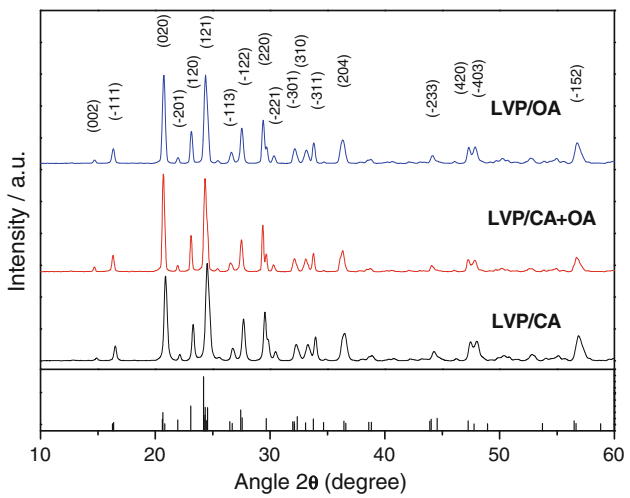

Fig. 1 XRD patterns of LVP/CA, LVP/CA+OA and LVP/OA samples in a 2θ range from 10 to 60°. For comparison the reflex positions based on single-phase LVP are given below (ICSD No. 96962)

of 1 μm. These particles are inter-grown onto and into carbonaceous residues having a size in the order of 10 μm. The carbonaceous residues are formed by the decomposition of the citric acid, which took place during the heat treatment of the precursor [9]. As reported in Table 1, the carbon content of the LVP/CA sample was equal to 25.3 %. The use of a mixture of citric acid and oxalic acid as the reducing agent leads to the formation of LVP particles in the order of 1–2 μm (Fig. 2b). The carbon content of the LVP/CA+OA sample was equal to 7.5 % and no big agglomerates of carbon particles were observed (Fig. 2b). Most likely, the lower content of carbon is due the decomposition of the oxalic acid (which displays high oxygen content) during the heat treatment applied for the synthesis. Such decomposition process might affect both the LVP and carbon morphology. The almost complete decomposition of the oxalic acid to volatile substances like CO_2, CO or H_2O even under protective gas atmosphere is shown by the LVP/OA sample. As indicated in Table 1, small amounts of carbonaceous residues (about 1.2 %) are detected in this sample, which also displays a lower hydrogen content as compared to the other samples. As shown in the SEM image (Fig. 2c), due to the low amount of carbon, the LVP particles of this sample grow together and form significantly larger agglomerates as compared to the other two samples mentioned above (which contain higher fractions of carbon).

As shown in Table 1, the amount of carbonaceous materials present in the samples affects their specific surface area. As indicated in the table, the sample LVP/CA, which displays the higher carbon content, shows the higher surface area (96 m^2 g^{-1}). The sample LVP/CA+OA, which features a lower carbon content as compared to the previous one has a specific surface area of 13 m^2 g^{-1}. The sample LVP/OA, which contains the lowest carbon content (about 1.2 %), displays significantly lower specific surface area (about 5 m^2 g^{-1}) as compared to the other two samples.

Figure 3 shows the voltammetric profiles of composite electrodes containing the three LVP samples. The CVs were carried out using a scan rate of 0.05 mV s^{-1}. As shown, the electrodes were investigated in two different voltage ranges: from 3.0 to 4.3 V versus Li/Li$^+$ and from 3.0 to 0.0 versus Li/Li$^+$. The first voltage range was selected in view of an application of the electrode as cathode for LIB, while the second voltage range for an application as anode. As visible in Fig. 3a, in the voltage range from 3.0 to 4.3 V versus Li/Li$^+$ the LVP electrodes show three peaks corresponding to the extraction/insertion of 0.5 (3.59/3.57 V vs. Li/Li$^+$), 0.5 (3.68/3.66 V vs. Li/Li$^+$) and 1.0 Li (4.09/4.04 V vs. Li/Li$^+$), respectively. As the peak currents were normalized to the active material masses (LVP without carbon coating) the values are comparable for all three samples. The LVP/CA electrodes,

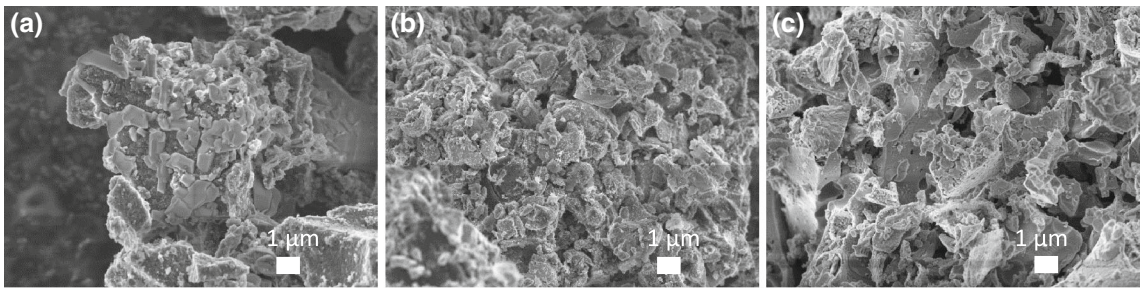

Fig. 2 SEM images of the **a** LVP/CA, **b** LVP/CA+OA and **c** LVP/OA samples

Table 1 Specific BET surface area, carbon and hydrogen content (combustion analysis) and L:V:P ratio (ICP-OES) of the three $Li_3V_2(PO_4)_3$ materials

	LVP/CA	LVP/CA+OA	LVP/OA
BET surface area ($m^2\ g^{-1}$)	96	13	5
Carbon content (%)	25.3	7.5	1.2
Hydrogen content (%)	0.7	0.4	0.11
L:V:P ratio	3:1.99:2.94	3:1.99:2.85	3:2.02:3.01

which display the highest carbon content, show the peaks with the highest specific currents and the smallest peak broadening. The LVP/CA+OA and LVP/OA display lower specific currents and a stronger peak broadening, as expected considering their lower carbon content. Nevertheless, it is important to note that the potential offset between the lithium insertion and extraction peaks is about 10 mV higher for the LVP/CA electrode than for the LVP/CA+OA electrode.

In the voltage range between 3.0 and 0.0 V versus Li/Li^+ the electrodes show four distinct peaks (2.02/1.96 V vs. Li/Li^+; 1.89/1.86 V versus Li/Li^+; 1.77/1.74 V vs. Li/Li^+; 1.71/1.67 V vs. Li/Li^+) each accounting for about 0.5 Li (Fig. 3b). These sharp peaks characterize a series of two-phase transitions. At lower potentials a solid-solution regime is observed, and in the voltage range between 1.6 and 0.0 V versus Li/Li^+ about 2 Li are reversibly inserted/extracted. It is interesting to observe that the LVP/CA electrodes display the highest specific current in the solid-solution regime, but the peaks of the two-phase transitions of the LVP/CA+OA electrodes with medium–high carbon content are more intense.

To gain further insight about the performance limiting factors of the investigated electrodes, GITT measurements were carried out (Fig. 4). The results of this investigation in the potential region between 3.0 and 4.3 V versus Li/Li^+ indicate that there is a strong influence of the carbon content, morphology and surface area on the diffusion coefficients. At the potentials in between the plateaus, the LVP/CA, LVP/CA+OA and LVP/OA show diffusion coefficients in the order of 10^{-10}, 10^{-11} and 10^{-12} $cm^2\ s^{-1}$, respectively. As shown, for all samples minima of the diffusion coefficients are observed in correspondence of the peak positions of the CVs (Fig. 3a). These minima have been found in several materials with a two-phase transition and have been associated to a strong interaction between the intercalated species and the host structure or a kind of order–disorder transition [22–24]. The minima show values ranging from 3×10^{-11} to 2×10^{-12} $cm^2\ s^{-1}$ for the LVP/CA electrodes, and values ranging from 3×10^{-13} to 6×10^{-14} $cm^2\ s^{-1}$ for the LVP/CA+OA and LVP/OA electrodes. It is important to note that as these diffusion coefficients were determined for a two-phase composition, they represent average diffusion coefficients resulting from the individual coefficients of the two phases and the phase boundary.

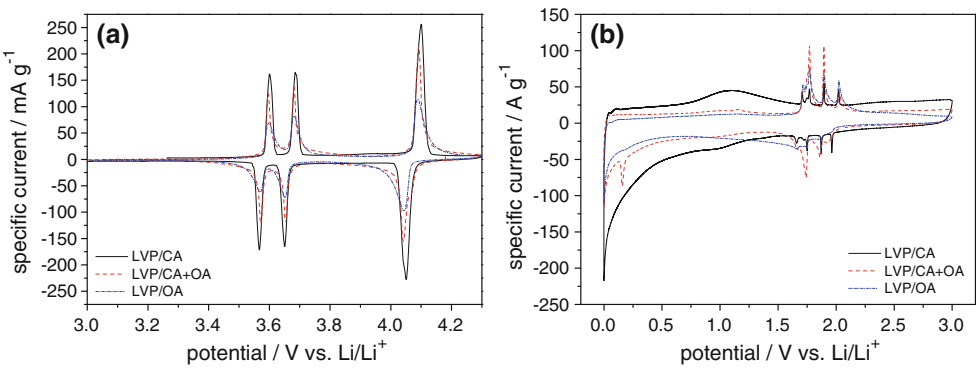

Fig. 3 Cyclic voltammograms of the LVP/CA, LVP/CA+OA and LVP/OA electrodes as **a** cathodes in the voltage range of 3.0–4.3 V versus Li/Li^+ at a scan rate of 0.05 mV s^{-1} and as **b** anodes in the voltage range of 3.0–0.0 V versus Li/Li^+ a scan rate of 0.05 mV s^{-1}

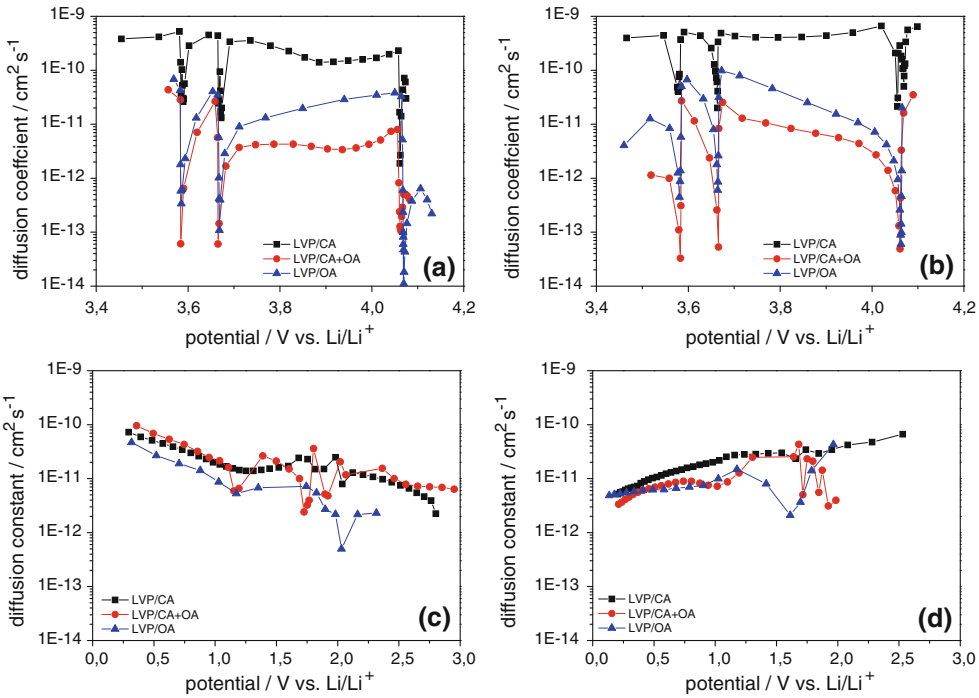

Fig. 4 GITT measurements of the LVP/CA, LVP/CA+OA and LVP/OA electrodes as cathodes in the voltage range of 3.0–4.3 V versus Li/Li$^+$ during **a** lithiation and **b** delithiation and as anodes in the voltage range of 3.0–0.0 V versus Li/Li$^+$ during **c** lithiation and **d** delithiation

Consequently, these values have to be regarded as apparent lithium diffusion coefficients. The values of the LVP/CA sample are in good agreement with previously published GITT results, which showed values in the order of 1.6×10^{-8} to 1.6×10^{-11} cm^2 s^{-1} [1]. A further confirmation of the reversibility of the lithium extraction/insertion process is the fact that similar values for diffusion coefficient could be obtained during charge and discharge, as seen in Fig. 4a, b.

It is important to point out that for the evaluation of the GITT data the geometric surface area of the electrodes (1.13 cm^2) was considered. Equation 1 illustrates that the calculation of the diffusion coefficient is normalized by the active surface, being the contact area between active material and electrolyte. To quantify the electrochemically active surface area the product of the BET surface area and the active material loading of the electrodes could be considered. However, the BET surface area is not equivalent to the electrochemically active surface area since it also includes surface area and pores formed by the (electrochemically inactive) carbonaceous material. Furthermore, not all the contact area between active material and electrolyte is electrochemically active, as already been reported in literature [23]. Therefore, to consider the specific surface area in the calculation might leads to underestimate the real diffusion coefficient of the material.

The evaluation of the GITT measurements in the potential range between 3.0 and 0.0 V versus Li/Li$^+$ revealed that there is clearly a two-phase behavior at the potentials corresponding to the CVs peaks. At these potentials, which correspond to the two-phase regions, diffusion coefficients comprise between 10^{-12} and 10^{-13} cm^2 s^{-1} were determined for the samples (Fig. 4c, d). In the potential range between 1.6 and 0.0 V versus Li/Li$^+$ solid-solution behavior is observed in the CV measurements. In this potential range all types of electrodes show diffusion coefficients comprise between 10^{-11} and 10^{-12} cm^2 s^{-1}. In this region, a clear trend of diffusion coefficients depending on the lithium content of the material is observed. As a matter of fact, during lithiation the diffusion coefficients increase steadily. This behavior may be explained by the fact that the number of lattice sites, which may accommodate additional lithium ions, is steadily decreased during the lithiation process. It was already confirmed by ex-situ XRD measurements that the material does not undergo a conversion reaction, but the monoclinic structure is preserved and only a small increase of the lattice constants takes place [8]. The results of this investigation are in line with the diffusion coefficients reported in literature for LVP-based anodes [10].

To check whether the samples show the expected electrochemical properties during lithiation and delithiation, galvanostatic experiments were carried out (Fig. 5). The three different LVP-based electrodes were subjected to charge/discharge C-rate experiments. The cathodes were examined in a voltage range between 3.0 and 4.3 V versus Li/Li$^+$ at C-rates of C/5, C/2, 1C, 2C, 5C and 10C. As in the investigated voltage range two lithium ions are available, a theoretical specific capacity of 133 mAh g^{-1} was calculated. At C/5, the electrodes LVP/CA, LVP/CA+OA

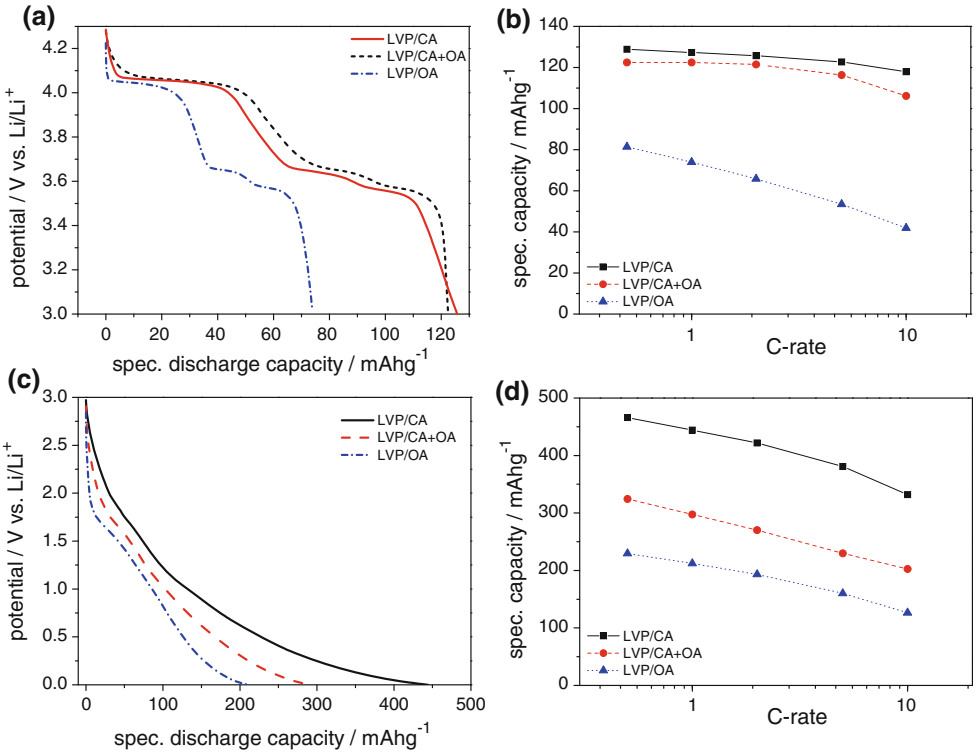

Fig. 5 Galvanostatic experiments carried out on LVP/CA, LVP/CA+OA and LVP/OA electrodes as cathodes in the voltage range of 3.0–4.3 V versus Li/Li^+ showing the **a** voltage profile at a C-rate of C/5 and the **b** evolution of the specific discharge capacity a C-rates of C/5, C/2, 1C, 2C, 5C and 10C as well as as anodes in the voltage range of 3.0–0.0 V versus Li/Li^+ showing the **c** voltage profile at a C-rate of C/5 and the **d** evolution of the specific discharge capacity a C-rates of C/5, C/2, 1C, 2C, 5C and 10C

and LVP/OA delivered capacity of 125.5, 122.5 and 74.0 mAh g^{-1}, respectively. Figure 5a displays the voltage profiles of the three different materials at C/5. As shown, although the LVP/CA-based electrode delivers the highest specific capacity the plateau potentials of this electrode are slightly decreased as compared to those of the electrode LVP/CA+OA. Moreover, the LVP/CA electrodes show a sloping profile progression below 3.5 V versus Li/Li^+. This sloping indicates that even at this low current density the material is not fully delithiated during the plateau, but more lithium is extracted at lower potentials. As this sloping effect is neither observed in the LVP/CA+OA electrodes nor in the LVP/OA electrodes, a lack of electronic conductivity (related with the carbon content) should not be the reason for this behavior. Most likely, the behavior of this electrode was caused by the presence of a thick layer of carbon surrounding the LVP active material. As the lithium ions have to pass though this carbon layer, a kind of kinetic hindrance is probably occurring. The low cut-off potential of 3.0 V versus Li/Li^+ allows the almost complete delithiation of the material despite its slower kinetics. However, the kinetic hindrance seems to be counterbalanced by the high electronic conductivity and even at increased C-rates the LVP/CA electrodes display the highest specific capacities (Fig. 5b). At a C-rate of 10C the electrodes containing LVP/CA, LVP/CA+OA and LVP/OA display specific capacities of 118.0, 106.2 and 41.9 mAh g^{-1}, respectively. A comparison with the values at C/5 reveals that the sample with the lowest carbon content, LVP/OA, shows the strongest relative capacity decrease among the three samples (51 % against 92 and 87 % for LVP/CA and LVP/CA+OA, respectively).

Figure 5c shows the voltage profiles of the three electrodes in the potential range between 3.0 and 0.0 V versus Li/Li^+. As mentioned in the introduction, the use of LVP as anode is possible since additional lithium ions can be inserted into the LVP structure. As described by Rui et al. about 2 lithium ions are accepted in a two-phase region comprise between 2.0 and 1.6 V versus Li/Li^+, and 2 more in the voltage region below 1.6 V versus Li/Li^+ in the form of a solid solution. During galvanostatic experiments the two-phase region can be identified by the presence of plateau in the voltage profiles. As shown in Fig. 5c, the plateau is clearly visible in the voltage profile of the LVP/OA, which contains the lowest carbon content among the samples, but it is hardly detectable on the profile of the LVP/CA electrode. This behavior may be originated by a kinetic hindrance caused by the high amount of carbon coating in the LVP/CA sample. Below 1.0 V versus Li/Li^+ the voltage profiles of the three LVP-based anodes are rather different. The LVP/OA electrodes show an almost constant slope until at about 0.2 V versus Li/Li^+. In this potential range the slope decreases significantly, indicating a stronger lithium uptake. In contrast to this behavior, the slope of the LVP/CA electrodes features no marked changes at this potential. It is important to take into account that high carbon content on the samples might smooth the electrochemical activity, but at the same time might

contribute to the capacity. The synthesis procedure, which involved maximal temperatures of 750 °C and carboxylic acids as precursors, is insufficient to produce high quality hard-/soft carbon or even graphite. However, the carbonaceous material present in the investigated LVP samples is able to reversibly accept/release lithium ions. The additional capacity related with this process is mainly occurring below 1.0 V versus Li/Li^+ and, therefore, it might partly covers the electrochemical response of the LVP-anode in this voltage region. For this reason the LVP/CA electrodes exceed the theoretical specific capacity of about 264 mAh g^{-1} (assuming $Li_xV_2(PO_3)_4$, $x = 3 - 7$, in the potential region 3.0–1.0 V versus Li/Li^+). The LVP/CA+OA electrodes display an intermediate behavior. The carbonaceous material contributes specific capacity but does not hide the features of the electrochemical activity of the LVP as strong as LVP/CA. The specific capacity of LVP/CA+OA at C/5 of 288 mAh g^{-1}. This value is only slightly higher than the theoretic specific capacity of the electrode. It is important to note that this amount of carbon coating enhances the electronic conductivity LVP, but does not contribute excessive amounts of specific capacity itself. The influence of the carbon coating and diffusion coefficient discussed above is also affecting the electrode behavior during test carried out at higher C-rate. As shown in Fig. 5d, at 10C the anodes containing LVP/CA, LVP/CA+OA and LVP/OA display specific capacities of 331.8, 202.7 and 126.5 mAh g^{-1}, respectively. The LVP/CA electrode is able to maintain high values of specific capacity even at increased C-rates because the amount of carbon coating increases the electronic conductivity of the material. This beneficial effect is not visible in the electrodes LVP/CA+OA and LVP/OA, which display lower carbon content.

4 Conclusions

This manuscript describes the influence of the carbon content and morphology of the material on the lithium ion diffusion properties of lithium vanadium phosphate. The diffusion coefficients were determined by GITT measurements, which revealed that $Li_3V_2(PO_4)_3$ displays promising diffusion coefficients, both as cathodic and as anodic material. Moreover, the results of this study clearly show that the porosity and the carbon content of the electrode materials is an important factor affecting the diffusion as well as the electrochemical performance of $Li_3V_2(PO_4)_3$. It was demonstrated that excessive carbon coating may lead to kinetic hindrances, but may also contribute specific capacity in anode materials in voltage regions below 1.0 V versus Li/Li^+.

Acknowledgments The authors wish to thank the University of Muenster, the Ministry of Innovation, Science and Research of North Rhine-Westphalia (MIWF) within the project "Superkondensator und Lithium-Ionen-Hybrid-Superkondensatoren auf der Basis ionischer Flüssigkeiten".

References

1. Whittingham MS (2004) Lithium batteries and cathode materials. Chem Rev 104:4271–4302
2. Song HK, Lee KT, Kim MG, Nazar LF, Cho J (2010) Recent progress in nanostructured cathode materials for lithium secondary batteries. Adv Funct Mater 20:3818–3834
3. Yin SC, Grondey H, Strobel P, Huang H, Nazar LF (2003) Charge ordering in lithium vanadium phosphates: electrode materials for lithium-ion batteries. J Am Chem Soc 125:326–327
4. Sun C, Rajasekhara S, Goodenough JB, Zhou F (2011) Monodisperse porous $LiFePO_4$ microspheres for a high power Li-ion battery cathode. J Am Chem Soc 133:2132–2135
5. Saıdi MY, Barker J, Huang H, Swoyer JL, Adamson G (2002) Electrochemical properties of lithium vanadium phosphate as a cathode material for lithium-ion batteries. Electrochem Solid-State Lett 5:A149–A151
6. Huang H, Yin SC, Kerr T, Taylor N, Nazar LF (2002) Nanostructured composites: a high capacity, fast rate $Li_3V_2(PO_4)_3$/carbon cathode for rechargeable lithium batteries. Adv Mater 14:1525–1528
7. Patoux S, Wurm C, Morcrette M, Rousse G, Masquelier C (2003) A comparative structural and electrochemical study of monoclinic $Li_3Fe_2(PO_4)_3$ and $Li_3V_2(PO_4)_3$. J Power Sour 119:278–284
8. Rui XH, Yesibolati N, Chen CH (2011) $Li_3V_2(PO_4)_3$/C composite as an intercalation-type anode material for lithium-ion batteries. J Power Sour 196:2279–2282
9. Böckenfeld N, Balducci A (2013) On the use of lithium vanadium phosphate in high power devices. J Power Sour 235:265–273
10. Rui XH, Yesibolati N, Li SR, Yuan CC, Chen CH (2011) Determination of the chemical diffusion coefficient of Li + in intercalation-type $Li_3V_2(PO_4)_3$ anode material. Solid State Ion 187:58–63
11. Rui XH, Ding N, Liu J, Li C, Chen CH (2010) Analysis of the chemical diffusion coefficient of lithium ions in $Li_3V_2(PO_4)_3$ cathode material. Electrochim Acta 55:2384–2390
12. Lee S, Park SS (2012) Atomistic simulation study of monoclinic Li_3V_2 $(PO_4)_3$ as a cathode material for lithium ion battery: structure, defect chemistry, lithium ion transport pathway, and dynamics. J Phys Chem C 116:25190–25197
13. Davis LJ, Goward GR (2013) Differentiating lithium ion hopping rates in vanadium phosphate versus vanadium fluorophosphate structures using 1D 6Li selective inversion NMR. J Phys Chem C 117:7981–7992
14. Chang C, Xiang J, Shi X, Han X, Yuan L, Sun J (2008) Hydrothermal synthesis of carbon-coated lithium vanadium phosphate. Electrochim Acta 54:623–627
15. Ren MM, Zhou Z, Gao XP, Peng WX, Wei JP (2008) Core-shell $Li_3V_2(PO_4)_3$@ C composites as cathode materials for lithium-ion batteries. J Phys Chem 112:5689–5693
16. Zhu XJ, Liu YX, Geng LM, Chen LB (2008) Synthesis and performance of lithium vanadium phosphate as cathode materials for lithium ion batteries by a sol–gel method. J Power Sour 184:578–582
17. Huang B, Fan X, Zheng X, Lu M (2011) Synthesis and rate performance of lithium vanadium phosphate as cathode material for Li-ion batteries. J Alloy Compd 509:4765–4768

18. Teng F, Hu ZH, Ma XH, Zhang LC, Ding CX, Yu Y, Chen CH (2013) Hydrothermal synthesis of plate-like carbon-coated $Li_3V_2(PO_4)_3$ and its low temperature performance for high power lithium ion batteries. Electrochim Acta 91:43–49
19. Rui XH, Li C, Chen CH (2009) Synthesis and characterization of carbon-coated $Li_3V_2(PO_4)_3$ cathode materials with different carbon sources. Electrochim Acta 54:3374–3380
20. Böckenfeld N, Placke T, Winter M, Passerini S, Balducci A (2012) The influence of activated carbon on the performance of lithium iron phosphate based electrodes. Electrochim Acta 76:130–136
21. Yin SC, Grondey H, Strobel P, Anne M, Nazar LF (2003) Electrochemical property: structure relationships in monoclinic Li_{3-y} V_2 $(PO_4)_3$. J Am Chem Soc 125:10402–10411
22. Prosini PP, Lisi M, Zane D, Pasquali M (2002) Determination of the chemical diffusion coefficient of lithium in $LiFePO_4$. Solid State Ion 148:45–51
23. Shaju KM, Subba Rao GV, Chowdari BVR (2003) EIS and GITT studies on oxide cathodes, O2-Li(2/3) + x (Co0.15Mn0.85) O 2 ($x = 0$ and 1/3). Electrochim Acta 48:2691–2703
24. Shaju KM, Rao GS, Chowdari BVR (2003) Li ion kinetic studies on spinel cathodes, Li (M1/6Mn11/6) O4 (M = Mn, Co., CoAl) by GITT and EIS. J Mater Chem 13:106–113